AD

AD-E402 982

Technical Report ARFSD-TR-03002

PREDICTING THE CAUSE OF FAILURE IN 120-mm MORTAR FINS

J. A. Cordes
H. Rand
D. Carlucci
L. Reinhardt
S. Kerwien

July 2003

US ARMY
TANK AUTOMOTIVE AND
ARMAMENTS COMMAND
ARMAMENT RDE CENTER

U.S. ARMY ARMAMENT RESEARCH, DEVELOPMENT AND ENGINEERING CENTER

Fire Support Armaments Center

Picatinny Arsenal, New Jersey

Approved for public release; distribution is unlimited.

REPORT DOCUMENTATION PAGE	*Form Approved* *OMB No. 0704-01-0188*

1. REPORT DATE (DD-MM-YYYY)	2. REPORT TYPE	3. DATES COVERED (*From – To)*
July 2003	Interim	January 2002 – January 2003

4. TITLE AND SUBTITLE

PREDICTING THE CAUSE OF FAILURE IN 120-mm MORTAR FINS

5a. CONTRACT NUMBER

5b. GRANT NUMBER

5c. PROGRAM ELEMENT NUMBER

6. AUTHORS

J. A. Cordes, H. Rand, D. Carlucci, L. Reinhardt, and S. Kerwien

5d. PROJECT NUMBER

5e. TASK NUMBER

5f. WORK UNIT NUMBER

7. PERFORMING ORGANIZATION NAME(S) AND ADDRESS(ES)
ARDEC, FSAC
Precision Munitions, Mines, & Demolition Division
(AMSTA-AR-STA-FSP-G)
Picatinny Arsenal, NJ 07806-5000

8. PERFORMING ORGANIZATION REPORT NUMBER

9. SPONSORING/MONITORING AGENCY NAME(S) AND ADDRESS(ES)
ARDEC, WECAC
Information Research Center (AMSTA-AR-WEL-TL)
Picatinny Arsenal, NJ 07806-5000

10. SPONSOR/MONITOR'S ACRONYM(S)

11. SPONSOR/MONITOR'S REPORT NUMBER(S)
Technical Report ARFSD-TR-03002

12. DISTRIBUTION/AVAILABILITY STATEMENT

Approved for public release; distribution is unlimited.

13. SUPPLEMENTARY NOTES

14. ABSTRACT
During 2002, approximately 1500 120-mm mortars were tested at Yuma Proving Grounds, Arizona. Of the 1500 rounds, seven fell short of the 7200-m range requirement. Inspection of the short rounds indicated that short rounds lost one or more fins.

This paper describes the structural analysis used to predict two proximal causes of failure. First, unequal pressure on one side of the fin can cause permanent bending, twisting, and breaking of the fin at its root. Second, internal pressure in the mortar tube can result in high hoop stresses where fracture failure can occur. Actual broken parts were consistent with one or the other predicted cause of failure.

15. SUBJECT TERMS

Mortar   Failure analysis   Yield   Fracture   Finite element analysis

16. SECURITY CLASSIFICATION OF:			17. LIMITATION OF ABSTRACT	18. NUMBER OF PAGES	19a. NAME OF RESPONSIBE PERSON J. A. Cordes
a. REPORT	b. ABSTRACT	c. THIS PAGE			19b. TELEPHONE NUMBER (Include area code) (973) 724-6147
U	U	U	SAR	15	

Standard Form 298 (Rev. 8/98)
Prescribed by ANSI Std. Z39.18

CONTENTS

FIGURES

INTRODUCTION

Millions of the Army's M9xx 120-mm mortars have been fielded. It is the Army's standard practice to conduct tests to verify the quality of the weapons prior to fielding of the production lot. In 2002, approximately 1500 mortars were tested at the Army's test facility in Yuma, Arizona. A number of mortars fell short of the 7200-m range requirement (ref. 1). All of the short rounds were missing one or more fins. It is not known whether the rounds that met range requirements had all of their fins intact.

An inspection of the test facility at Yuma yielded dozens of broken fin sections, probably from years of tests. Most of the broken parts consisted of bent and twisted fins (fig. 1). Some broken parts had flat fins and part of the cylinder (fig. 2).

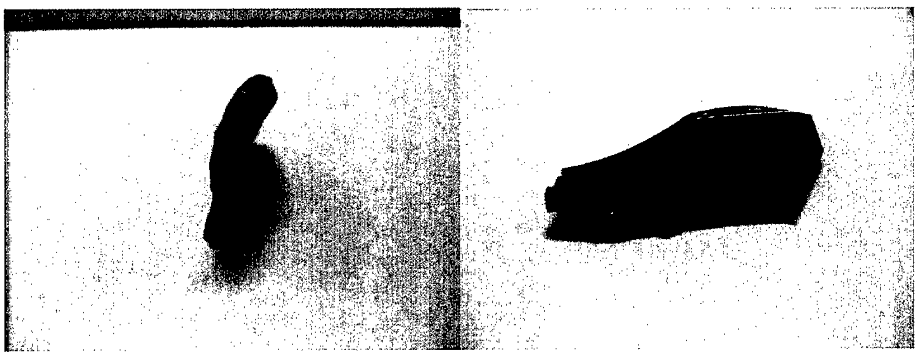

Figure 1
Two broken and deformed mortar-fins

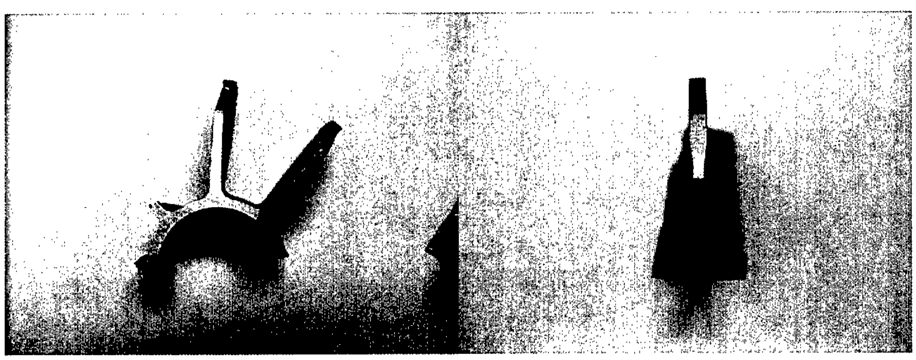

Figure 2
Two broken fin parts, flat fin plus cylindrical part

This paper describes the structural analyses used to determine the proximal causes of failures in the 120-mm mortar. Finite element analysis was done with a number of different loading cases. Several high stress regions were predicted for different applied loads.

The analyses indicated two types of failures under two different loading conditions. The proximal cause of failures at the fin root (fig. 1) is unequal pressure on one side of the fin. This higher pressure can cause bending, twisting, yielding, and/or ripping of the fin. The proximal cause of failure between fins (fig. 2) is a defect at a high-hoop stress region that results in fracture failure. The fracture failure occurs from an internal pressure in the fin cylinder. Yielding is probably not visible.

STRUCTURAL ANALYSIS

Geometry

The geometry of the two-part tail-assembly was imported from the Pro Engineer (ProE) drawings (fig. 3). The assembly consists of two tubular sections: an inner perforated tube and an outer tube with eight fins. The inner perforated section is about 225-mm long, has an inner diameter of about 26-mm, and an outer diameter of 36-mm. Ignition cartridges are wrapped around the perforated section. The fin section was about 58-mm long, with an outer diameter of about 42 mm, and an inner diameter of about 36 mm. The two parts are press-fit together. The maximum interference fit, based on the tolerances on the drawing, is about 0.11 mm. The fin section had the failures.

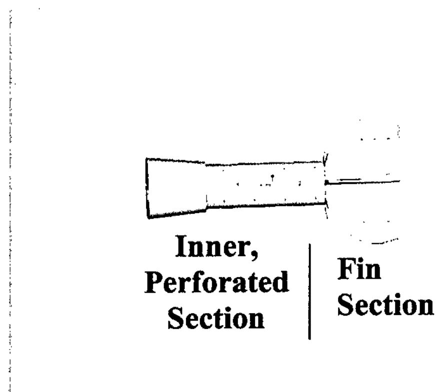

Figure 3
Solid rendering of the tail section of the 120-mm mortar

Finite Element Model

The two part tail-assembly was de-featured and analyzed using the general-purpose, finite-element program ABAQUS (ref. 2). The inner perforated section was de-featured to eliminate fillets and holes. The fin section was analyzed with little de-featuring. Fillets at the fin root and fillets near the press-fit were retained. The ProE geometry was altered in ABAQUS to have the maximum interference. All analyses were nonlinear and included the press fit.

One-eighth model was used to model the two parts (fig. 4). Both cylindrical sections were modeled using 8-node brick elements. In addition to the symmetry constraints, an axial constraint was used on both parts.

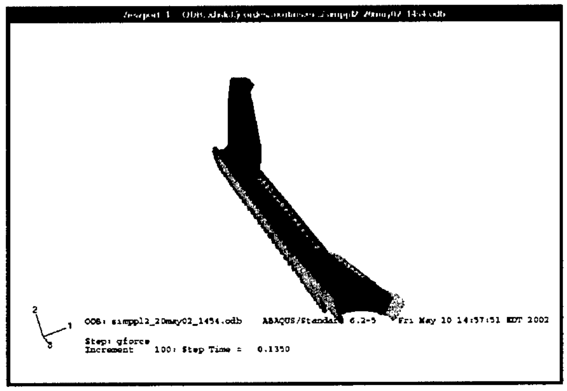

Figure 4
Finite element mesh and boundary, 1/8-model

Material

Both parts of the tail assembly were extruded from aluminum. Young's Modulus was 73,023 MPa, Poisson's ratio was 0.3, and the mass density was 2.3-gm/cm^3. The perforated section was modeled as a linear-elastic material. The fin section was modeled as an elastic-plastic material. Points from a tensile test of a fin were used to model the fin part (fig. 5). The engineering yield and ultimate strength were 464 and 502 MPa. ABAQUS uses the true stress and strain, 466 MPa for yield and 538 MPa for ultimate tensile strength.

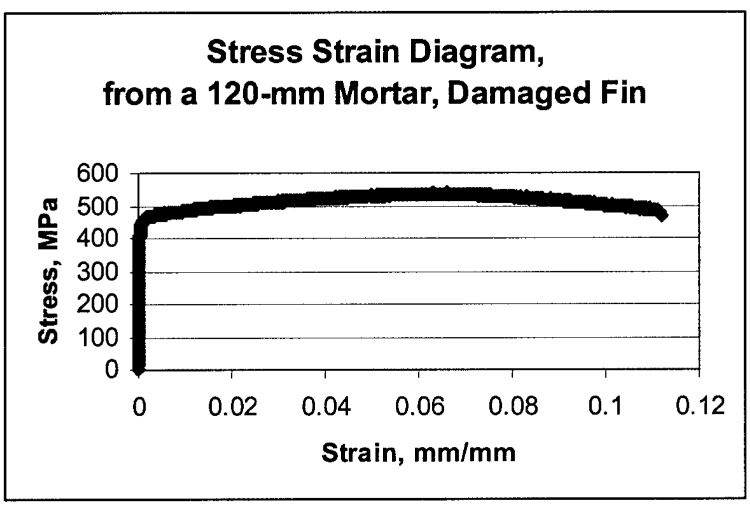

Figure 5
Stress/strain diagram from damaged fin

A fracture analysis was done on the fin section following analysis. The fracture toughness for the fin-section is estimated to be 17.9 MPa$\sqrt{m}$.

RESULTS

Table 1 summarizes the load cases that were evaluated. The first step initialized displacements and stresses due to the press fit. In case 2, a uniform internal pressure was applied to the inside of the perforated tube (fig. 6a). The magnitude of the internal pressure, 98 MPa, was determined from experimental measurement. In load step 3, a uniform pressure was applied to the outside of the assembly. In load step 4, pressure was applied to one side of the fin (fig. 7a). No yielding resulted from load cases 1 and 3 and stresses were lower than for cases 2 and 4.

Table 1
Load cases

Case	Load	Load MPa	Maximum Mises MPa	Plastic strain mm/mm	Plasticity at
1	Press fit	0.0	301.2	None	None
2	Internal pressure	98.0	478.4	0.0017	Inner radius, under fin
3	External pressure	10.4	234.2	0.0017	No additional
4	Fin pressure	3.5	683.0	0.048	Fin back

The internal pressure of 98 MPa, load case 2 from table 1, resulted in three, high-stress regions (fig. 6b). There are high von Mises stresses directly under the fin and at the inner diameter of the cylinder, at the fin fillet on the outside of the fin cylinder, and midway between the fins on the inside of the fin tube. Yielding was predicted directly under the fin on the inside of the cylinder. The plastic region did not go through the thickness of the cylinder and the von Mises stress was below the ultimate tensile strength of the aluminum.

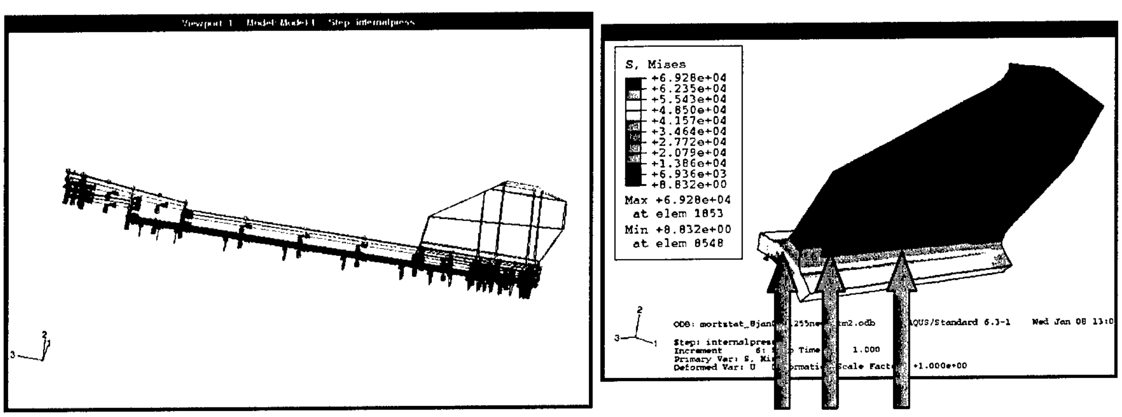

Figure 6
Internal pressure on fin assembly, 98 MPa

Critical crack sizes were predicted for the three high-stress regions shown in figure 6b. The smallest critical cracks resulted from the longitudinal cracks opened by the hoop stresses. For load, the 98-MPa internal pressure, the smallest critical flaw on the inside of the cylinder, was estimated at 0.18 mm (0.007 in.). Along the outside of the cylinder, the smallest critical crack size was estimated at 0.23 mm (0.009 in.). As shown in figure 2, several of the broken fins had failure modes consistent with fracture failure. The failure surface was rough and without discernable yielding of the fins or fin cylinder.

Figure 7a shows load case 4, an unequal pressure on one side of the fin. A pressure of 1.4 MPa resulted in yielding of the fin near the root. A pressure of 2.1 MPa resulted in von Mises stresses exceeding the ultimate tensile strength of the aluminum (figure 7b in units psi). At the 2.1-MPa pressure, the plastic zone extended through the fin thickness, indicating probable tearing of the fin at this location. Numerous examples of broken and twisted fins were consistent with the deformation and stresses shown in figure 7b.

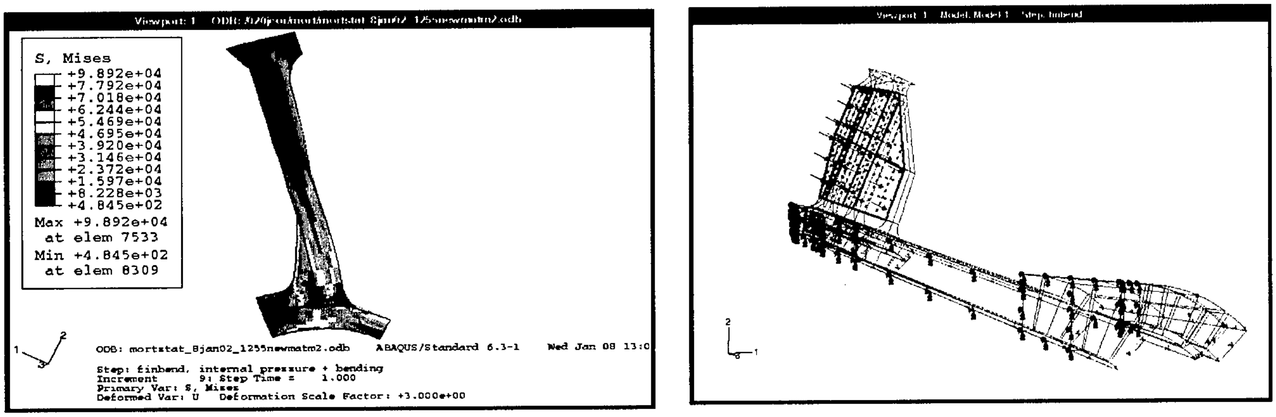

Figure 7
Load case 4: pressure on one side of fin

Additional evidence of unequal pressure as a proximal cause of failure occurred in recent short-rounds. In the broken short-rounds in figure 8, two adjacent damaged fins appear to be twisting away from the same spot, indicting high pressure between two fins. In figure 8a, note the fins at 10:00 and 12:00 seem to be twisting in opposite directions. Similarly the damaged fins in figure 8b seem to be twisting away from one another. Note the fins at 4:00 and 6:00 in figure 8b.

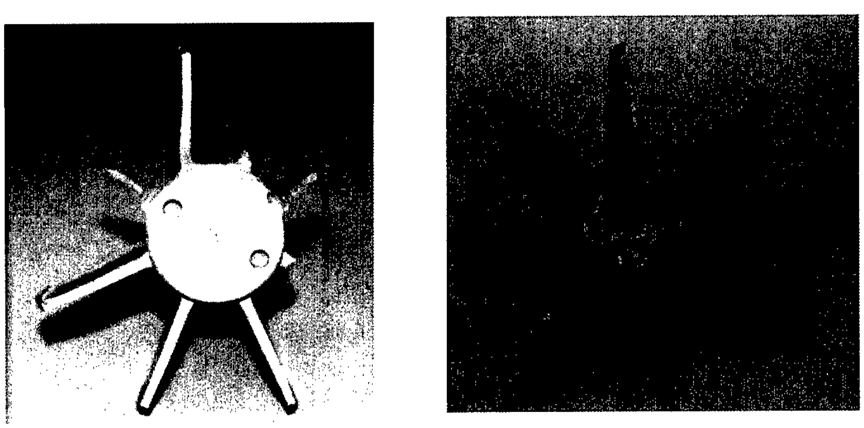

Figure 8
Evidence of high unequal pressure between two fins

CONCLUSIONS

The analysis indicated that a fracture could occur with large internal pressures at critical defects. The smallest crack size was predicted with longitudinal cracks on the inside of the fin cylinder. This type of defect is consistent with scoring due to assembly at the press fit. Evidence of scoring was found in some broken parts, but it was not clear that scoring had caused a specific failure. However, the broken parts shown in figure 2 are consistent with the high stress regions in figure 6b.

The analysis indicated that permanent deformation and failure can result from pressure on one side of the fin. The broken fins in figure 1 were consistent with the high stress pattern predicted in figure 7b.

RECOMMENDATIONS, ON-GOING, AND FUTURE WORK

Six-sigma techniques are being used to assess the manufacturing and assembly process. The goal is to reduce the size and number of scoring defects on the inside of the fin cylinder.

A test program was initiated to determine if unequal pressure is occurring on one side of the fins. Instrumentation of rounds is in progress. Results should provide a dozen pressure time curves over different fins for different charge distributions. The input will by used to determine dynamic reaction of the fins and to verify that unequal pressure is occurring in some cases.

REFERENCES

1. The Mortar Book, Product Manager Mortar Systems, Picatinny Arsenal, pg. 3-41, May 1998.

2. ABAQUS, version 6.2, Hibbitt, Karlsson & Sorenson, Inc., Pawtucket, RI, 2003.

DISTRIBUTION LIST

Commander
Armament Research, Development and Engineering Center
U.S. Army Tank-automotive and Armaments Command
ATTN: AMSTA-AR-WEL-TL (2)
AMSTA-AR-GCL
AMSTA-AR-FSP-G
AMSTA-AR-FSA, M. Chiefa
AMSTA-AR-FSA-M, J. Feneck
SFAE-AMO-CAS-MS, P. Burke
SFAE-AMO-CAS, W. DeMassi
P. Serao
COL Sledge
SFAE-AMO
AMSTA-AR-FSP-B (4)
Picatinny Arsenal, NJ 07806-5000

Defense Technical Information Center (DTIC)
ATTN: Accessions Division
8725 John J. Kingman Road, Ste 0944
Fort Belvoir, VA 22060-6218

Director
U.S. Army Materiel Systems Analysis Activity
ATTN: AMXSY-EI
392 Hopkins Road
Aberdeen Proving Ground, MD 21005-5071

Commander
Soldier and Biological/Chemical Command
ATTN: AMSSB-CII, Library
Aberdeen Proving Ground, MD 21010-5423

Director
U.S. Army Research Laboratory
ATTN: AMSRL-CI-LP, Technical Library
Bldg. 4600
Aberdeen Proving Ground, MD 21005-5066

Chief
Benet Weapons Laboratory, CCAC
Armament Research, Development and Engineering Center
U.S. Army Tank-automotive and Armaments Command
ATTN: AMSTA-AR-CCB-TL
Watervliet, NY 12189-5000

Director
U.S. Army TRADOC Analysis Center-WSMR
ATTN: ATRC-WSS-R
White Sands Missile Range, NM 88002

Commander
Naval Air Warfare Center Weapons Division
1 Administration Circle
ATTN: Code 473C1D, Carolyn Dettling (2)
China Lake, CA 93555-6001

Chemical Propulsion Information Agency
ATTN: Accessions
10630 Little Patuxent Parkway, Suite 202
Columbia, MD 21044-3204

GIDEP Operations Center
P.O. Box 8000
Corona, CA 91718-8000